ghg GREENHOUSE GASES SCIENCE AND TECHNOLOGY SCI

Influence of CO_2-wettability on CO_2 migration and trapping capacity in deep saline aquifers

Emad A. Al-Khdheeawi[1*], Stephanie Vialle[2], Ahmed Barifcani[1], Mohammad Sarmadivaleh[1], Stefan Iglauer[1]

[1] Department of Petroleum Engineering, Curtin University, 6151 Kensington, Western Australia.

[2] Department of Exploration Geophysics, Curtin University, 6151 Kensington, Western Australia.

Corresponding author: Emad A. Al-Khdheeawi (e.al-khdheeawi@postgrad.curtin.edu.au)

Abstract

CO_2 migration and trapping capacity in deep saline aquifers are highly influenced by various rock and fluid parameters. One of the key parameters, which, however, has received little attention, is CO_2-wettability. We thus simulated the behavior of a CO_2 plume in a deep saline aquifer as a function of rock wettability and predicted various associated CO_2 migration patterns and trapping capacities. We clearly show that CO_2-wet reservoirs are most permeable for CO_2; CO_2 migrates furthest upwards and the plume has a "candle-like" shape, while in a water-wet reservoir the plume is more compact and "rain-drop" shaped. Furthermore, higher residual trapping capacities are achieved in water-wet rock, while solubility trapping is more efficient in CO_2-wet rock. We thus conclude that rock wettability has a highly significant impact on both CO_2 migration and trapping capacities and that water-wet reservoirs are preferable CO_2 sinks due to their higher storage capacities and higher containment security.

Keywords

CO_2-rock wettability, trapping mechanisms, plume migration, 3D reservoir simulations, Carbon dioxide, saline aquifers

1. Introduction

CO_2 capture and storage (CCS) is considered an one effective method to mitigate greenhouse gas emission into the atmosphere by collecting CO_2 from large point sources and injecting it into deep geological formations.[1,2]. Storage sites, however, need to be screened for storage effectiveness, with prospective targets including unminable coal beds, deep saline aquifers and depleted hydrocarbon reservoirs.[3-8]. Among all these types of CO_2 storage sites, deep saline aquifers are considered more suitable, because they have the largest CO_2 storage capacity and the widest geographical spread .[6,9] For safety and efficiency reasons, CO_2 is injected at depths greater than 800 m, so that CO_2 remains in a supercritical (sc) state.[1,3,10,11] However, scCO_2 - although denser than CO_2 gas - is buoyant compared to formation water and migrates upwards; this migration can be minimized and CO_2 can be prevented from escaping to the atmosphere by four main trapping mechanisms, namely structural,[11-13] residual,[10,14,15] dissolution,[16-18] and mineral trapping.[19-21]

Many factors affect the efficiency and capacity of the main CO_2 trapping mechanisms: temperature,[22] vertical to horizontal permeability ratio,[23] cap rock properties, [13] fault-seal behaviour,[24, 25] or reservoir heterogeneity.[26] One factor, which has received little attention, is the CO_2-wettability of the rock,[27,28] ; we show here that CO_2-wettability has a dramatic impact on storage capacities, CO_2 plume migration patterns and CO_2 containment security. It is also important to note that CO_2-rock wettability can vary tremendously. Indeed, water contact angles between 0° (strongly water-wet) and 170° (strongly CO_2-wet) have been measured,

where CO_2-wettability mainly depends on the surface chemistry, and to a lesser extend on temperature, pressure and brine composition.[13,27,29-39]

Wettability, as it has been previously shown in laboratory experiments (at the mm to cm scale), has a significant effect on residual trapping (cp.[15, 40-42]) and structural trapping.[12, 13] However, despite this laboratory-scale evidence, the effect of wettability on reservoir scale processes and associated storage capacity and containment security predictions has received little attention[27] and generally, though the wettability is incorporated in the pilot projects modelling via relative permeability curves and multiphase flow, the values are poorly constrained.

In this paper, we investigate the influence of CO_2 wettability of rocks on CO_2 plume migration, CO_2 mobility and the capacity of residual and solubility trapping and demonstrate its key importance. For this purpose we performed multiphase flow reservoir simulations on a hectometre scale formation using 5 relative permeability curves (including hysteresis) that represent 5 characteristic wettability scenarios from strongly water-wet to strongly CO_2-wet.

2. Methodology

2.1 Numerical model

We built a 3D homogeneous reservoir-scale model (Figure 1) using the nonisothermal multicomponent multiphase flow simulator TOUGH2[43] with the fluid property module ECO2M to model the thermodynamic and thermophysical properties of the H_2O-NaCl-CO_2 mixtures that includes super- and sub-critical conditions, as well as phase changes between liquid and gaseous CO_2.[44] ECO2M is a tabular EOS and it depends on Altunin's correlations[45] to compute the molar volumes of CO_2 (including the CO_2 dissolved in brine). The amount of dissolved CO_2 was used to assess dissolution trapping.[16-18] The aquifer characteristics are

summarized in Table 1; [23,46] the top of the aquifer is at 800 m depth. It is overlayed by a lower permeability unit (10^{-6} D compared to 1 D for that of the reservoir) typical of that of mudstones,[47,48] and is modelled as a water-wet formation, for all wettability scenarios considered in this paper (including the CO_2-wet models): this unit constitutes thus a barrier preventing the CO_2 from migrating to the surface. Reservoir pressure and temperature were set to 8 MPa (at 800 m depth) and 313 K (40° C), respectively. The pressure followed the hydrostatic gradient (10 MPa/km),[49] while temperature conditions were isothermal. Dirichlet boundary conditions for pressure (i.e. constant pressure) were assigned on the outer boundary grid cells by applying a large volume multiplier (10000).[50]

CO_2 was injected into the reservoir at a constant rate of 3.171 kg/sec (100,000 tCO_2/ yr) for all modelled scenarios; this is an injection rate similar to that of the Ordos CCS demonstration project in China[51] and Tomakomai CCS demonstration project in Japan.[52] CO_2 was injected at a depth of 1150m (i.e. near the bottom of the reservoir and at the centre of the model) over a 1 year period (i.e. a total of 100000 tons of CO_2 were injected). Subsequently the CO_2 injection well was shut down and the behaviour of the CO_2 plume was simulated for the following 10 year period ("storage period"). Five different wettability scenarios were analysed, namely strongly water-wet, weakly water-wet, intermediate-wet, weakly CO_2-wet and strongly CO_2-wet with an assumed contact angle (Θ) of (0°, 70°, 110°, 130°, and 170°), respectively.[27,39] Note that all wettability states are physically possible and they may prevail in a specific storage reservoir, as mentioned in the introduction.

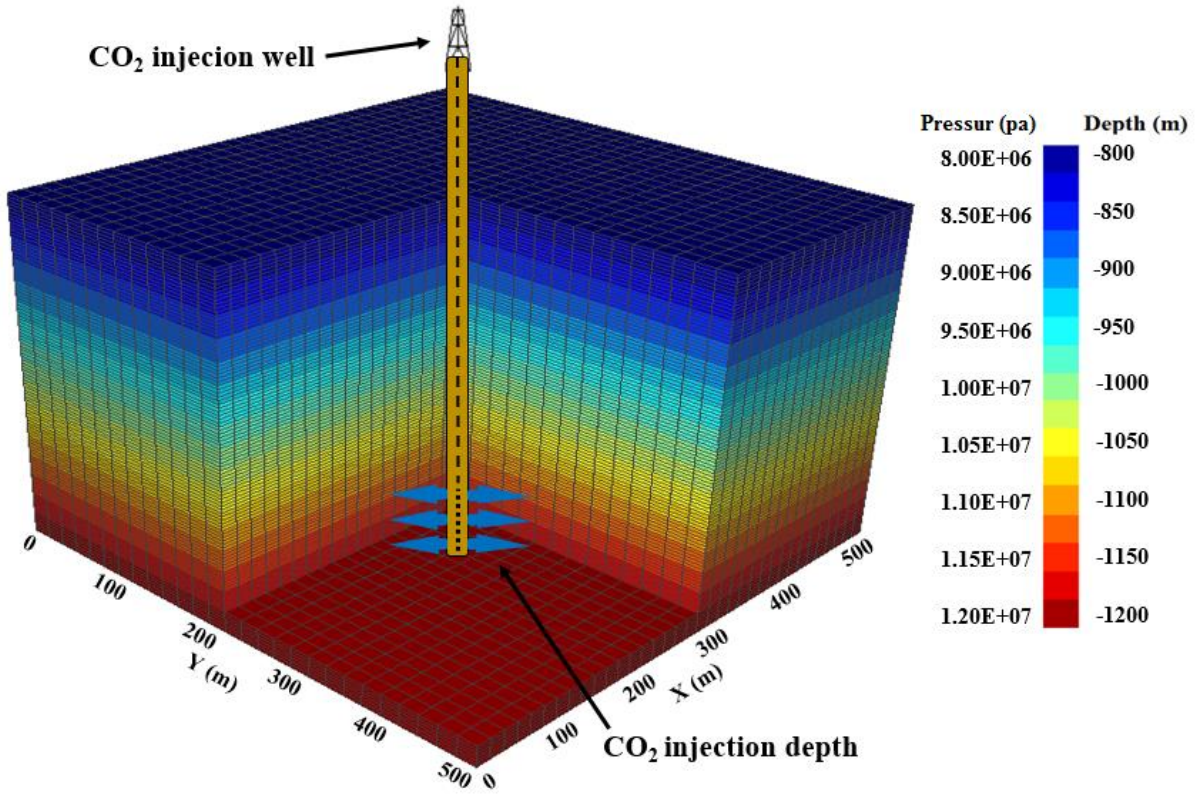

Figure 1. A sketch of the 3-D model including location of the injection well, model dimensions, and initial pressure.

Table 1: Reservoir model characteristics.

Property	**Value**
Length	500 m
Width	500 m
Thickness	400 m
Cell number	35 x 27 x 100 (94500 cells in total)
Top depth of the reservoir	-800 m
Bottom depth of the reservoir	-1200 m
Reservoir temperature (isothermal)	313 K(40^{0} C)
Initial pressure (at depth -800 m)	8 MPa
Initial pressure (at depth -1200 m)	12 MPa

Salinity	15% NaCl by weight
Horizontal permeability	1000 mD
Vertical to horizontal permeability ratio	0.1
Top seal permeability	10^{-3} mD
Porosity	0.25
Initial water saturation	100%

2.2 Wettability simulation

CO_2-wettability is an atomistic phenomenon as it is determined by intermolecular forces between CO_2, brine and rock.[31,32,35,36,53] Thus, to perform hectometre-scale reservoir simulations, an upscaling mechanism is required; here we directly implement the effect of wettability into the relative permeability and capillary pressure curves.[54-59]

Specifically, we use McCaffery and Bennion's[55] relative permeability curves to construct the curves for the 5 wettability scenarios investigated in this study and adjusted them based on Craig's criteria.[60] This procedure consists in an adjustment of the values of end point saturations, i.e. water saturations where CO_2 and water relative permeabilities (k_{rg} and k_{rw}) are equal, and relative permeabilities at water floodout (i.e. the condition when the rock reached its maximum water saturation). According to Craig's criteria, and for a reservoir permeability of 1000 mD, the residual water saturation (S_{wr}) should be less than 15% in strongly CO_2-wet rocks, and should range between 20%-50% in strongly water-wet rocks. In addition, the water saturation where k_{rg} and k_{rw} are equal should be higher than 50% in a strongly water-wet reservoir, while it should be less than 50% in a strongly CO_2-wet reservoir. Moreover, the k_{rw} during the storage period should be less than 30% in the strongly water-wet formation, and it should range between 50%-100% in the strongly CO_2-wet reservoir. All above conditions were applied during construction of the relative permeability curves used in this study, which

are displayed in Figure 2. The curves were then fitted with the Van Genuchten-Mualem model[61, 62] for implementation into the computer code:

$$k_{rw} = \sqrt{S^*}\left\{1-\left(1-[S^*]^{1/\lambda}\right)^{\lambda}\right\}^2 \quad \text{if} \quad S_w < S_{ws} \qquad \text{(Eq.1)}$$

$$k_{rw} = 1 \quad \text{if} \quad S_w = 1 \qquad \text{(Eq.2)}$$

$$k_{rg} = 1 - k_{rw} \quad \text{if} \quad S_{gr} = 0 \qquad \text{(Eq.3)}$$

$$k_{rg} = \left(1-\hat{S}\right)^2\left(1-\hat{S}^2\right) \quad \text{if} \quad S_{gr} > 0 \qquad \text{(Eq.4)}$$

and $S^* = (S_w - S_{wr})/(S_{ws} - S_{wr})$, $\hat{S} = (S_w - S_{wr})/(1 - S_{wr} - S_{gr})$ (Eq.5)

where:

k_{rg} = relative permeability for gas, k_{rw} = relative permeability for water

S_{gr} = residual gas saturation, S_w = water saturation

S_{ws} = saturated (maximum) water saturation (= 1), S_{wr} = residual water saturation.

λ = fitting parameter (pore size distribution index).

Initially, k_{rw} is set to 1 and k_{rg} to 0, which corresponds to full (100%) water saturation. During CO_2 injection (dashed black lines in Figure 2), k_{rw} reduces gradually, while k_{rg} increases until it reaches a maximum at the irreducible water saturation (S_{wr}). During the storage period (CO_2 injection has ceased, represented by red lines in Figure 2), k_{rg} reduces and k_{rw} increases until residual gas saturation (S_{gr}) is reached. Note that the endpoint saturations (S_{wr}, S_{gr}) depend on wettability[15,40-42,54,60] and Moreover, lower water-wettability shifts the k_{rw} curve upwards, and the k_{rw}-k_{rg} cross-over point moves towards the left (i.e. to a lower water saturation value).[60] Furthermore, note that S_{gr} is also a function of the initial CO_2 saturation[10,63,64] and porosity.[15]

Figure 3 presents the capilarry pressure curves used in this study for the 5 different wettability scenarios. These curves has been developed by referring on previous studies,[58,59] (which look at the wettability-capillary pressure relationship) and by using the Van Genuchten-Mualem model [(61, 62)]:

$$(P_{cap}) = P_0 \left([S^*]^{-1/\lambda} - 1\right)^{1-\lambda} \quad \text{(Eq.6)}$$

$$S^* = (S_w - S_{wr})/(S_{ws} - S_{wr}) \quad \text{(Eq.7)}$$

where:

P_c = CO_2-water capillary pressure, P_o = capillary pressure scaling factor, S_{ws} = maximum (saturated) water saturation, S_{wr} = residual water saturation, λ = pore size distribution index.

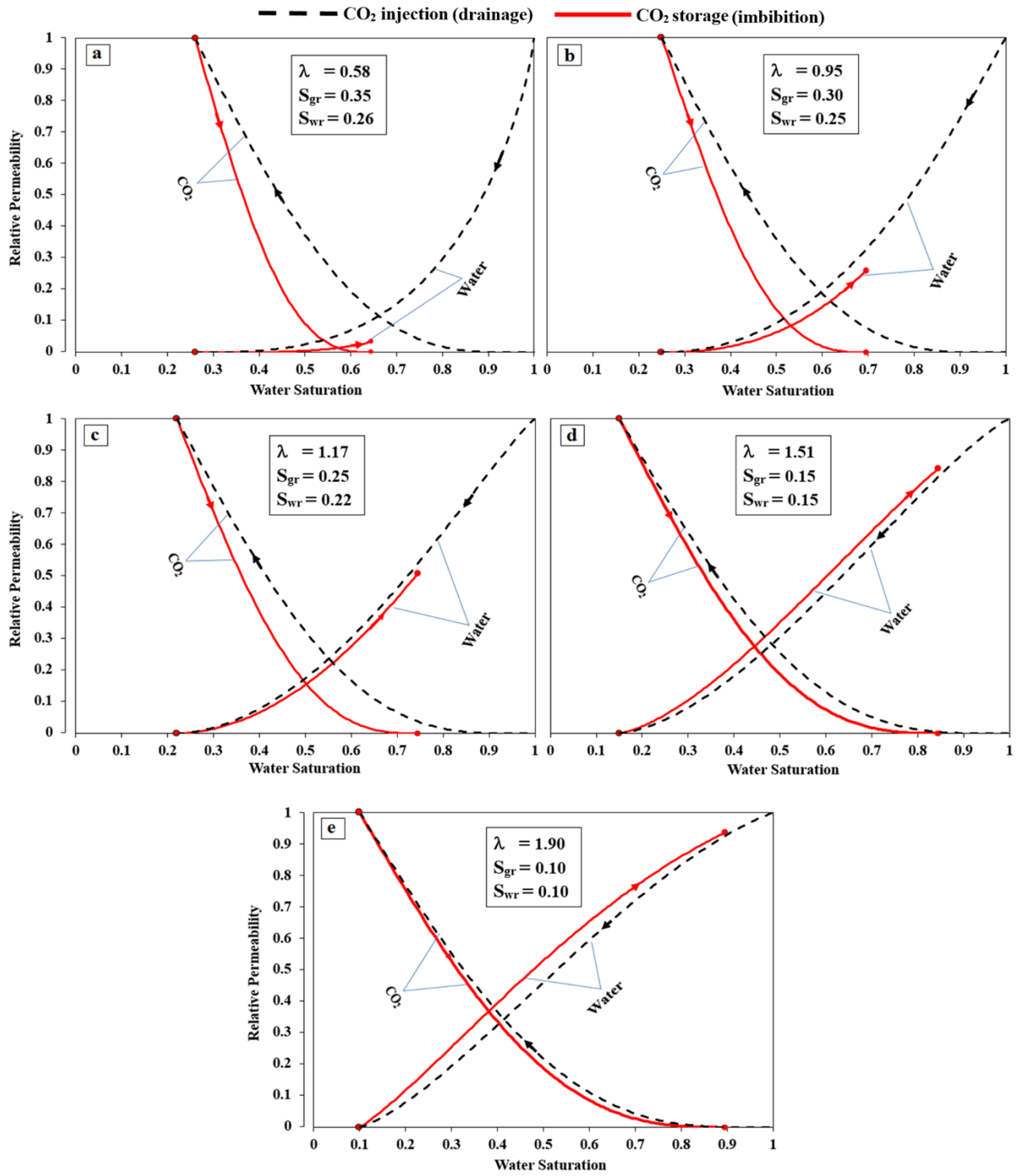

Figure 2. Relative permeability curves for the five different rock wettabilities investigated: a) strongly water-wet; b) weakly water-wet; c) intermediate-wet; d) weakly CO_2-wet; e) strongly CO_2-wet. See section 2.2 for the construction of these curves.

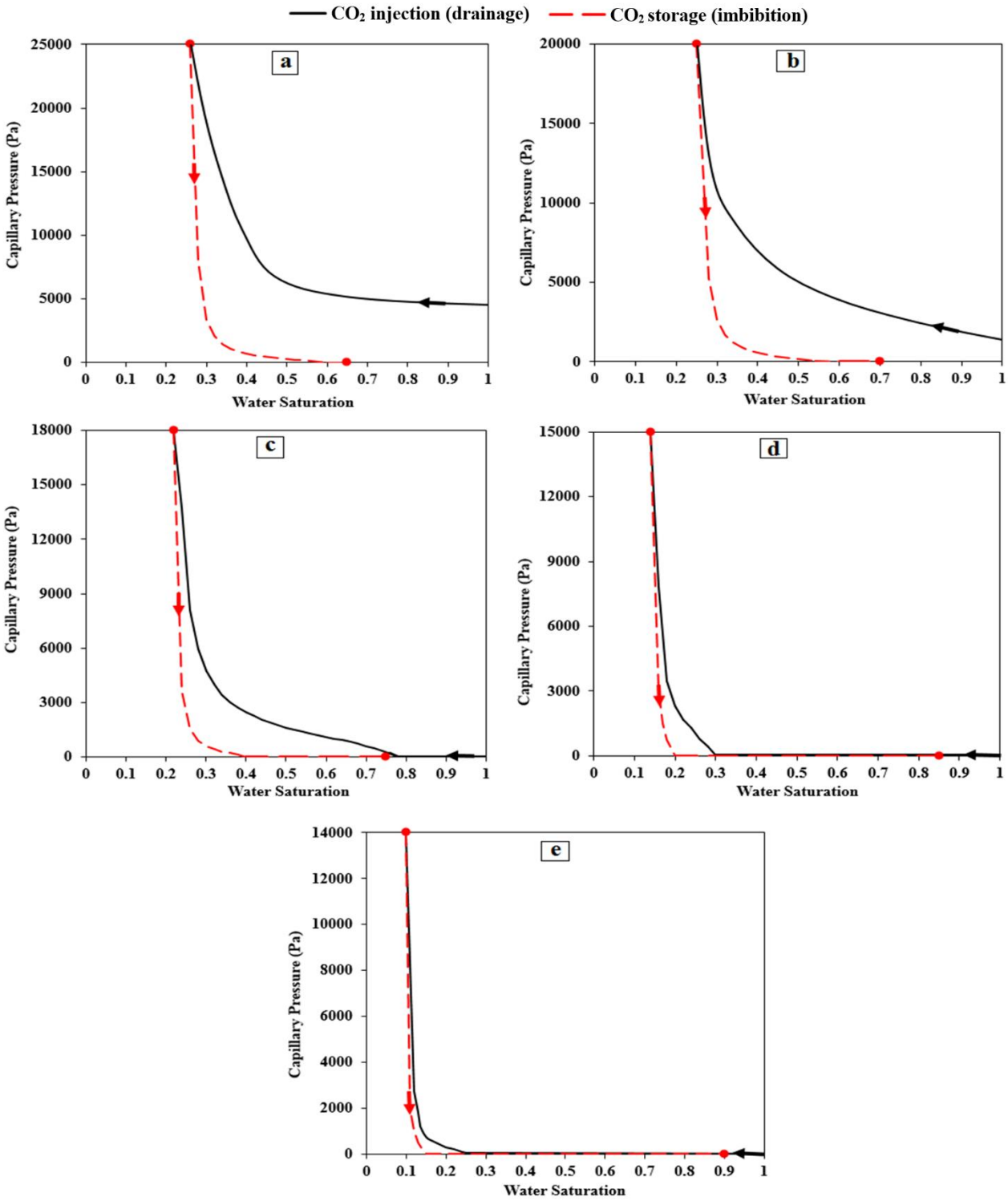

Figure 3. Capillary pressure curves for the five different rock wettabilities investigated: a) strongly water-wet; b) weakly water-wet; c) intermediate-wet; d) weakly CO_2-wet; e) strongly CO_2-wet. See section 2.2 for the construction of these curves.

3. Results and discussion

3.1 Influence of wettability on CO_2 plume migration and shape

Clearly wettability has a significant influence on the CO_2 migration pattern. Figure 4 displays 3D views of the CO_2 plume for the 5 wettability scenarios described above and at various times after the end of the injection. The CO_2 plume moves upwards much more rapidly in the strongly CO_2-wet rock scenario, while it is best retained near the injection well in the strongly water-wet reservoir; this is quantified in Table 2, where the depth reached by the (free) CO_2 plume, as well as the total CO_2 vertical migration distance, are reported. Furthermore, rock wettability has a drastic impact on the shape of the CO_2 plume; while the plume is much more compact and "raindrop-like" in a water-wet reservoir, it has a (vertically) elongated "candle-like" shape in the CO_2-wet reservoir (Figure 4).

The underlying reason why the CO_2 plume moves upwards much more rapidly in strongly CO_2-wet rock is because of the wettability influence on relative permeability and capillary pressure on dual phase systems. Wettability is also the reason why the spreading patterns are different in CO_2-wet and water-wet reservoirs. Recall that the endpoint saturations (S_{wr}, S_{gr}) depend on wettability[15, 40-42,54,60] A CO_2 migration and plume extension are highly dependent on S_{gr}, [3,14,65] CO_2 migration rate increases and the plume expands spatially with smaller S_{gr} values. Figure 2, which shows the variation of S_{gr} with wettability, that the lowest S_{gr} (10%) is associated with the strongly CO_2-wet condition, while the highest S_{gr} (35%) is found in the strongly water-wet reservoir. We conclude that CO_2-wettability dramatically affects CO_2 plume migration both in time and space.

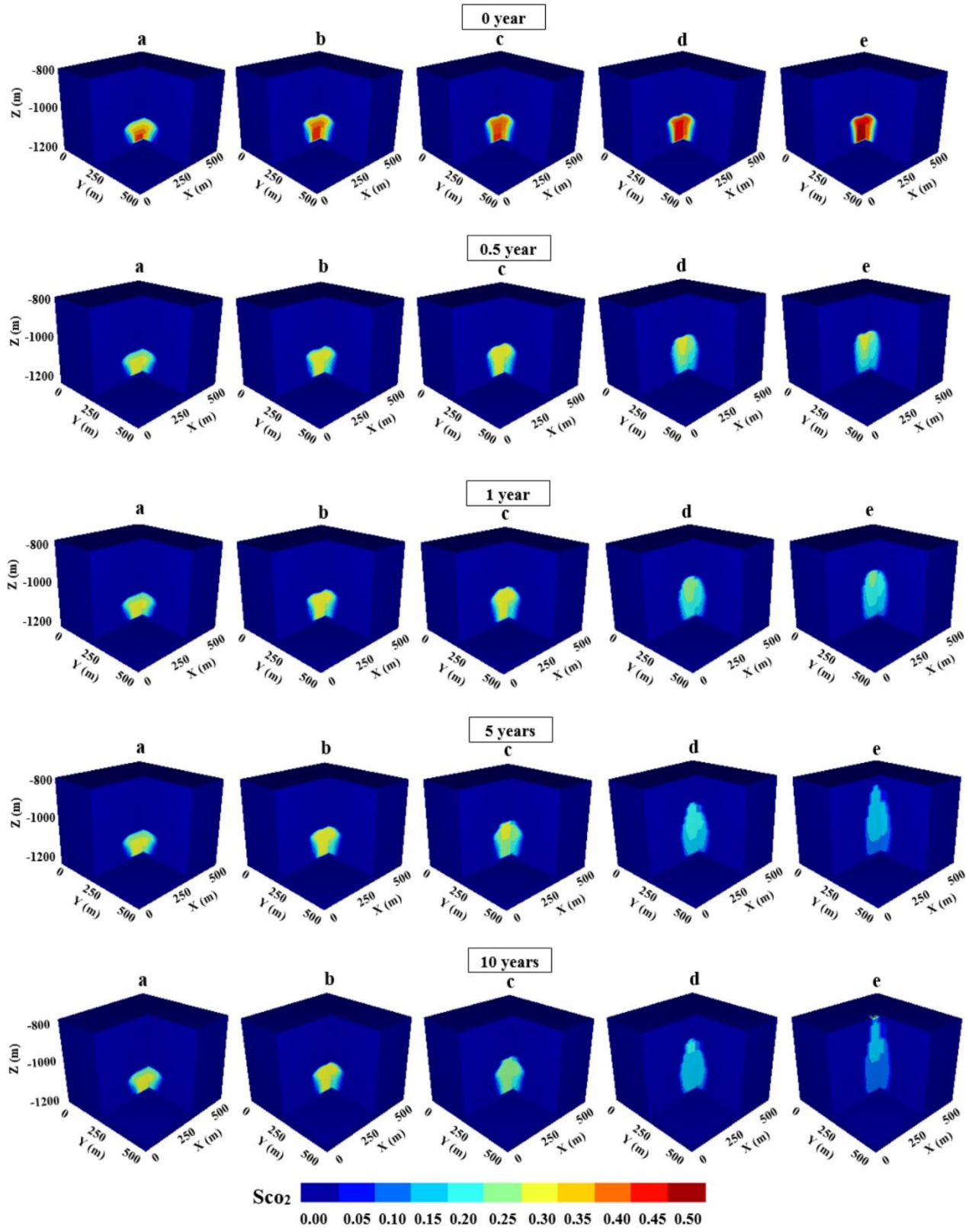

Figure 4. 3D views of the CO_2 plume as a function of storage time (i.e times since the stop of injection) and wettability: a) strongly water-wet; b) weakly water-wet; c) intermediate-wet; d) weakly CO_2-wet; e) strongly CO_2-wet. Z= model height; X, Y= model length and width.

Table 2. Depth[a] reached and vertical migration distance of CO_2 plume after the end of the storage period (10 years) for the five different wettability scenarios investigated.

Wettability	Depth reached by the free CO_2 plume (m)	Vertical migration distance of the free CO_2 plume (m)[b]
Strongly water-wet	-1034	116
Weakly water-wet	-1014	136
Intermediate-wet	-978	172
Weakly CO_2-wet	-889	261
Strongly CO_2-wet	-800[c]	350

[a]CO_2 injection depth was at (-1150 m).

[b]CO_2 plume migration distance measured from the top of the perforated interval.

[c]In the case of the strongly CO_2-wet reservoir, CO_2 reached the top of the model (-800 m) after only 8 years; CO_2 then flowed laterally beneath the caprock.

3.2 Influence of wettability on storage mechanisms

We further analyse the impact of wettability on the CO_2 storage mechanisms by distinguishing (at the end of the 10 year storage period) and quantifying the amount of dissolved (in brine) CO_2, mobile CO_2 and residual CO_2. Residual CO_2 is CO_2 that is entrapped in the pore space of the rock by capillary forces[15,40-42] and that has thus been immobilized.

The percentage of trapped CO_2, either by dissolution or by residual trapping and of mobile (free) CO_2 during the storage period is displayed in Figure 5 for all wettability cases; corresponding percentages are reported in Table 3 for the end of the storage period (i.e. after 10 years). Generally for all wettability cases, the percentage of trapped CO_2, either by dissolution trapping or residual trapping, increased over time during the storage period, and consequently the amount of free $scCO_2$ decreased (Figure 5), which is consistent with previous studies.[14,26,27,66,67]

In the case of a strongly water-wet rock, most (99.5%) of the CO_2 is already trapped at the beginning of the storage period, either by dissolution (~18%) or by residual trapping (~81%). This is due to the relatively small amount of CO_2 injected and the high residual CO_2 saturation (S_{gr} = 35%) in the strongly water-wet rock compared with lower residual CO_2 saturation in the less water-wet scenarios (reducing to S_{gr} = 10% in the strongly CO_2-wet case (see Figure 2)); thus the CO_2 plume in the water-wet rock appears stagnant in Figure 4 (changes in dissolved CO_2 are insignificant). With increasing CO_2-wettability the amount of residual CO_2 trapping dropped dramatically, from ~80% in case of strongly water-wet rock to ~50% in case of strongly CO_2-wet rock, 10 years after the injection has stopped. This is due to the lower capillary forces in CO_2-wet rock and the resulting lower S_{gr}.[41,42] Recall that S_{gr} strongly depends on the wettability[15,40-42,54,60], see Figure 2. Consequently, residual trapping capacities strongly depend on wettability as wettability strongly impacts S_{gr} and therefore the overall residual CO_2 saturation.

On the contrary, dissolution trapping was more efficient in strongly CO_2-wet rock, with ~18 % for strongly water-wet rock compared to ~29% for strongly CO_2-wet rock after 10 years storage time. It is important to mention here that this difference in dissolution trapping between CO_2-wet and water-wet reservoirs is because the CO_2 plume moves faster through the CO_2-wet reservoir and spreads out more. The more the plume spreads , however, the larger the CO_2-brine interface becomes. And a larger CO_2-brine interface leads to more dissolution trapping.[3,14,65]

Thus, our results show that there is a highly significant impact of wettability on the ratio of mobile to residual CO_2, and a significant effect on dissolution trapping.

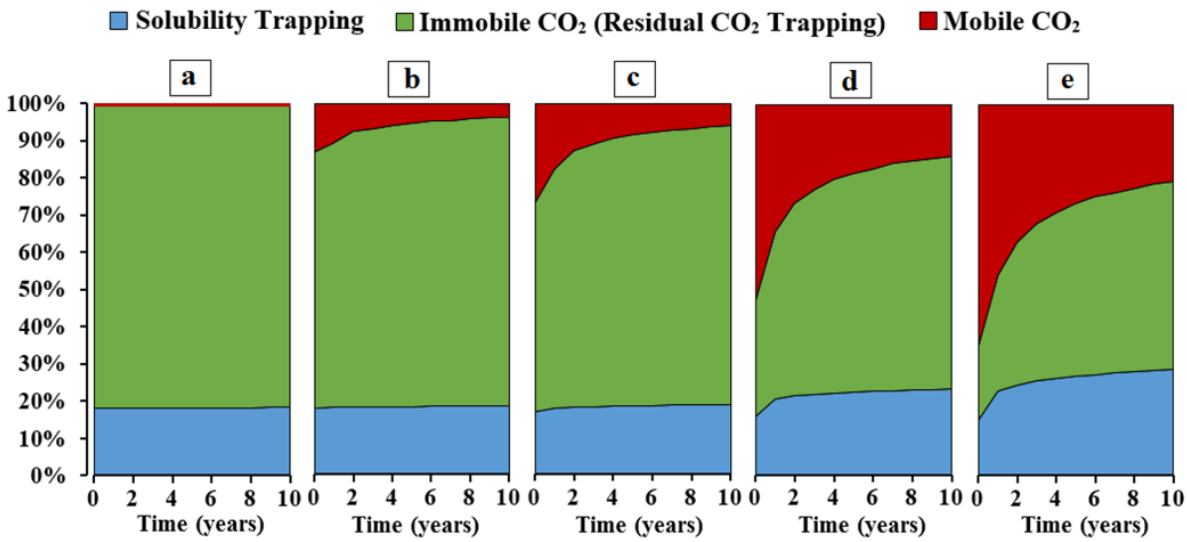

Figure 5. Percentage of free and trapped CO_2 for the 5 different rock wettabilities investigated (dissolution trapping is in blue, residual trapping is in green and mobile CO_2 is in red): a) strongly water-wet; b) weakly water-wet; c) intermediate-wet; d) weakly CO_2-wet; e) strongly CO_2-wet.

Table 3. Percentage of free and trapped CO_2 at the end of the storage period (10 years) for the five different wettabilities investigated

Wettability	**Mobile CO_2 %**	**Solubility trapped CO_2 %**	**Residually trapped CO_2 %**
Strongly water-wet	0.5	18.3	81.2
Weakly water-wet	3.9	18.5	77.6
Intermediate-wet	6.0	18.7	75.3
Weakly CO_2-wet	13.8	23.2	63.0
Strongly CO_2-wet	20.7	28.6	50.7

4. Conclusions

CO_2-wettability of rocks can vary tremendously, from strongly water-wet to strongly CO_2-wet (cp. the recent review by Iglauer et al.[27] and the reference list in the introduction of this study). Such wettability variation has been previously shown, in laboratory experiments, to strongly influence residual trapping[15, 40-42] and structural trapping.[12, 13]

Here, for the first time, we systematically analysed the effect of rock wettability on the CO_2 plume behaviour in an idealized reservoir and computed the amount of mobile and trapped CO_2 (by both residual and solubility trapping mechanisms) at the hectometre-scale via reservoir simulations.

Our simulations clearly indicate that CO_2 is best retained in water-wet rock, while CO_2-wet reservoirs are relatively much more permeable to CO_2. Furthermore, the shape of the CO_2 plume is also strongly affected by wettability, the plume is much more compact in case of water-wet rock, while it is vertically elongated in CO_2-wet rock. Moreover, in our example case study over a 10 year storage period, the amount of residually trapped CO_2 is significantly higher in water-wet rock. On the contrary, dissolution trapping is more effective in CO_2-wet rock.

In summary, wettability significantly changes migration patterns and storage capacities, which is directly relevant to CO_2 geo-storage projects. Moreover, we conclude that strongly water-wet reservoirs are preferable CO_2 sinks due to their higher storage capacities and superior containment security. This result has important implications for designing geoengineering solutions aiming at increasing CO_2 storage especially in situations where an efficient and continuous seal is absent (e.g. the South West Hub project in Western Australia.[68] Recent laboratory experiments indeed show that intermediate-wet and CO_2-wet reservoirs can be treated (e.g. with silica nanofluid,[69]) to render them strongly water-wet.

Nomenclature

EOS = Equation of state

D = Darcy

k_h = Horizontal permeability [mD]

k_{rg}= Relative permeability for gas [-]

k_{rw}= Relative permeability for water [-]

k_v = Vertical permeability [mD]

mD = Millidarcy

P = Pressure [Pa, MPa]

P_o = capillary pressure scaling factor

P_c = CO_2-water capillary pressure

S_{gr} = Residual gas saturation [-]

S_w =Water saturation [-]

S_{ws} = Saturated water saturation [-]

S_{wr} = Residual water saturation [-]

T= Temperature [K, °C]

Θ = Contact angle

λ = fitting parameter (pore size distribution index).

References

1. Pruess K, Xu T, Apps J, Garcia J. Numerical Modeling of Aquifer Disposal of CO_2. *SPE J* **8**(01): 49-60 (2003).

2. Holloway S. Underground sequestration of carbon dioxide—a viable greenhouse gas mitigation option. *Energy* **30** (11): 2318-2333 (2005).

3. Metz B, Davidson O, De Coninck H, Loos M, Meyer L. IPCC, 2005: *IPCC special report on carbon dioxide capture and storage*. Prepared by Working Group III of the

Intergovernmental Panel on Climate Change. Cambridge, United Kingdom and New York, NY, USA, 442 pp. (2005).

4. Iglauer S. Carbon capture and storage with a focus on capillary trapping as a mechanism to store carbon dioxide in geological porous media. *Adv Multiphase Flow Heat Transfer* **3**:177-197 (2012).

5. Juanes R, Spiteri E, Orr F, Blunt M. Impact of relative permeability hysteresis on geological CO_2 storage. *Water Resour Res* **42**(12): 1-13 (2006)

6. Bachu S. Sequestration of CO_2 in geological media: criteria and approach for site selection in response to climate change. *Energy Convers Manage* **41**(9):953-70 (2000).

7. Bickle MJ. Geological carbon storage. *Nature Geosci* **2**(12):815-818 (2009).

8. Sakurovs, R. and Lavrencic, S. Contact angles in CO_2-water-coal systems at elevated pressures. Int J Coal Geol. **87**(1): 26-32 (2011).

9. Lackner KS. A guide to CO_2 sequestration. *Science* **300**(5626):1677-1678 (2003).

10. Pentland CH, El-Maghraby R, Iglauer S, Blunt MJ. Measurements of the capillary trapping of super-critical carbon dioxide in Berea sandstone. *Geophys Res Lett* **38**(6):1-4 (2011).

11. Hesse M, Orr F, Tchelepi H. Gravity currents with residual trapping. *J Fluid Mech* **611**(1):35-60 (2008).

12. Naylor M, Wilkinson M, Haszeldine R. Calculation of CO_2 column heights in depleted gas fields from known pre-production gas column heights. *Mar Petrol Geol* **28**(5):1083-1093 (2011).

13. Iglauer S, Al-Yaseri AZ, Rezaee R, Lebedev M. CO_2 wettability of caprocks: Implications for structural storage capacity and containment security. *Geophys Res Lett* **42**(21):9279-9284 (2015).

14. Kumar A, Noh MH, Ozah RC, Pope GA, Bryant SL, Sepehrnoori K, et al. Reservoir simulation of CO_2 storage in deep saline aquifers. *Spe J* **10**(03):336-48 (2005).

15. Iglauer S, Paluszny A, Pentland CH, Blunt MJ. Residual CO_2 imaged with X-ray micro-tomography. *Geophys Res Lett* **38**(21):1-6 (2011).

16. Lindeberg E, Wessel-Berg D. Vertical convection in an aquifer column under a gas cap of CO_2. *Energy Convers and Manage* **38**:S229-S234 (1997).

17. Spycher N, Pruess K, Ennis-King J. CO_2-H_2O mixtures in the geological sequestration of CO_2. I. Assessment and calculation of mutual solubilities from 12 to 100 C and up to 600 bar. *Geochim Cosmochim Ac* **67**(16):3015-3031(2003).

18. Iglauer S. *Dissolution trapping of carbon dioxide in reservoir formation brine-a carbon storage mechanism*: INTECH Open Access Publisher (2011).

19. Bachu S, Gunter W, Perkins E. Aquifer disposal of CO_2: hydrodynamic and mineral trapping. *Energy Convers Manage* **35**(4):269-279 (1994).

20. Xu T, Apps JA, Pruess K. Numerical simulation of CO_2 disposal by mineral trapping in deep aquifers. *Appl Geochem* **19**(6):917-936 (2004).

21. Gaus I. Role and impact of CO 2–rock interactions during CO_2 storage in sedimentary rocks. *Int J Greenhouse Gas Control* **4**(1):73-89 (2010).

22. Ofori, A. E., & Engler, T. W. Effects of CO_2 sequestration on the petrophysical properties of an aquifer rock. *SPE Paper 147166, Proceeding of the Canadian*

Unconventional Resources Conference, Calgary, Alberta, Canada (November 15–17, 2011).

23. Basbug, B., Gumrah, F., & Oz, B. Simulating the Effects of Deep Saline Aquifer Properties on CO_2 sequestration. *Paper presented at the Petroleum Society's 6th Canadian International Petroleum Conference*, Calgary, Alberta, Canada (June 7 – 9, 2005).

24. Bretan, P., Yielding, G., Mathiassen, O. M. and Thorsnes, T. Fault-seal analysis for CO_2 storage: an example from the Troll area, Norwegian Continental Shelf. *Petrol Geosci* 17(2): 181-192 (2011).

25. Yielding, G., Lykakis, N. and Underhill, J. R. The role of stratigraphic juxtaposition for seal integrity in proven CO_2 fault-bound traps of the Southern North Sea. *Petrol Geosci* 17(2): 193-203 (2011).

26. Gershenzon NI, Ritzi RW, Dominic DF, Soltanian M, Mehnert E, Okwen RT. Influence of small-scale fluvial architecture on CO_2 trapping processes in deep brine reservoirs. *Water Resour Res* **51**(10):8240-8256 (2015).

27. Iglauer S, Pentland C, Busch A. CO_2 wettability of seal and reservoir rocks and the implications for carbon geo-sequestration. *Water Resour Res* **51**(1):729-774 (2015).

28. Vialle S, Druhan JL, Maher K. Multi-phase flow simulation of CO_2 leakage through a fractured caprock in response to mitigation strategies. *Int J Greenhouse Gas Control* **44**:11-25 (2016).

29. Chiquet P, Broseta D, Thibeau S. Wettability alteration of caprock minerals by carbon dioxide. *Geofluids* **7**(2):112-122 (2007).

30. Broseta D, Tonnet N, Shah V. Are rocks still water-wet in the presence of dense CO_2 or H2S? *Geofluids* **12**(4):280-294 (2012).

31. Iglauer S, Mathew M, Bresme F. Molecular dynamics computations of brine–CO_2 interfacial tensions and brine–CO_2–quartz contact angles and their effects on structural and residual trapping mechanisms in carbon geo-sequestration. *J Colloid Interf Sci* **386** (1):405-414 (2012).

32. McCaughan J, Iglauer S, Bresme F. Molecular dynamics simulation of water/CO_2-quartz interfacial properties: Application to subsurface gas injection. *Energy Proc* **37**:5387-5402 (2013).

33. Saraji S, Goual L, Piri M, Plancher H. Wettability of supercritical carbon dioxide/water/quartz systems: Simultaneous measurement of contact angle and interfacial tension at reservoir conditions. *Langmuir* **29**(23):6856-6866 (2013).

34. Iglauer S, Salamah A, Sarmadivaleh M, Liu K, Phan C. Contamination of silica surfaces: Impact on water–CO_2–quartz and glass contact angle measurements. *Int J Greenhouse Gas Control* **22**:325-328 (2014).

35. Chen C, Wan J, Li W, Song Y. Water contact angles on quartz surfaces under supercritical CO_2 sequestration conditions: Experimental and molecular dynamics simulation studies. *Int J Greenhouse Gas Control* **42**:655-665 (2015).

36. Javanbakht G, Sedghi M, Welch W, Goual L. Molecular Dynamics Simulations of CO_2/Water/Quartz Interfacial Properties: Impact of CO_2 Dissolution in Water. *Langmuir* **31**(21):5812-5819 (2015).

37. Sarmadivaleh M, Al-Yaseri AZ, Iglauer S. Influence of temperature and pressure on quartz–water–CO_2 contact angle and CO_2–water interfacial tension. *J Colloid Interf Sci* **41**:59-64 (2015).

38. Al-Yaseri AZ, Lebedev M, Barifcani A, Iglauer S. Receding and advancing (CO_2+ brine+ quartz) contact angles as a function of pressure, temperature, surface roughness, salt type and salinity. *J Chemical Thermodyn* **93**:416-423 (2016).

39. Arif M, Barifcani A, Lebedev M, Iglauer S. Structural trapping capacity of oil-wet caprock as a function of pressure, temperature and salinity. *Int J Greenhouse Gas Control* **50**:112-120 (2016).

40. Andrew M, Bijeljic B, Blunt MJ. Pore-scale imaging of geological carbon dioxide storage under in situ conditions. *Geophys Res Lett* **40** (15):3915-3918 (2013).

41. Chaudhary K, Bayani Cardenas M, Wolfe WW, Maisano JA, Ketcham RA, Bennett PC. Pore-scale trapping of supercritical CO_2 and the role of grain wettability and shape. *Geophys Res Lett* **40** (15):3878-3882 (2013).

42. Rahman T, Lebedev M, Barifcani A, Iglauer S. Residual trapping of supercritical CO_2 in oil-wet sandstone. *J Colloid Interf Sci* **469**:63-68 (2016).

43. Pruess K, Oldenburg C, Moridis G. TOUGH2 User's Guide Version 2. Lawrence Berkeley National Laboratory (1999).

44. Pruess K. ECO2M: a TOUGH2 fluid property module for mixtures of water, NaCl, and CO_2, including super-and sub-critical conditions, and phase change between liquid and gaseous CO_2. Lawrence Berkeley National Laboratory (2011).

45. Altunin V. Thermophysical properties of carbon dioxide. Moscow (in Russian): *Publishing House of Standards*, Moscow Russia (1975).

46. Jahangiri HR, Zhang D. Effect of spatial heterogeneity on plume distribution and dilution during CO_2 sequestration. *Int J Greenhouse Gas Control* **5**(2):281-293 (2011).

47. Dewhurst, D. N., Aplin, A. C. and Sarda, J. P. Influence of clay fraction on pore-scale properties and hydraulic conductivity of experimentally compacted mudstones. *J Geophys Res-Sol Ea* **104**(B12): 29261-29274 (1999).

48. Yang, Y.L., Aplin, A.C. Permeability and petrophysical properties of 30 natural mudstones. *J Geophys Res* 112 (B03206):1-14 (2007).

49. Dake LP. Fundamentals of reservoir engineering: *Elsevier* (1983).

50. Nghiem, L., Shrivastava, V., Tran, D., Kohse, B., Hassam, M., & Yang, C. Simulation of CO_2 storage in saline aquifers. *SPE Paper 125848, Proceeding of SPE/EAGE Reservoir Characterization & Simulation Conference*, Abu Dhabi, UAE (October 19-21, 2009).

51. Xiuzhang W. Shenhua Group's carbon capture and storage (CCS) demonstration. *Mining Report* **150**(1-2):81-84 (2014).

52. Tanaka Y, Abe M, Sawada Y, Tanase D, Ito T, Kasukawa T. Tomakomai CCS Demonstration Project in Japan, 2014 Update. *Energy Proc* **63**:6111-6119 (2014).

53. Liu S, Yang X, Qin Y. Molecular dynamics simulation of wetting behavior at CO_2/water/solid interfaces. *Chinese Sci Bull* **55**(21):2252-2257 (2010).

54. Anderson WG. Wettability literature survey part 5: the effects of wettability on relative permeability. *J Petrol Technol* **39**(11):1453-1468 (1987).

55. McCaffery F, Bennion D. The Effect of Wettability on Two-Phase Relative Pemeabilities. *J Can Petrol Technol* **13**(04): 42-53 (1974).

56. Levine JS, Goldberg DS, Lackner KS, Matter JM, Supp MG, Ramakrishnan T. Relative Permeability Experiments of Carbon Dioxide Displacing Brine and Their Implications for Carbon Sequestration. *Environ Sci Technol* **48**: 811-818 (2014)

57. Krevor S, Pini R, Zuo L, Benson SM. Relative permeability and trapping of CO_2 and water in sandstone rocks at reservoir conditions. *Water Resour Res* **48**(2):1-16 (2012).

58. Anderson, W. G. Wettability literature survey-part 4: Effects of wettability on capillary pressure. *J Petrol Technol* 39 (10):1283-1300 (1987).

59. Morrow, N. R. Capillary pressure correlations for uniformly wetted porous media. *J Can Petrol Technol*. 15(04): 49-69 (1976).

60. Craig FF. *The reservoir engineering aspects of waterflooding*: Richardson, TX: Henry L. Doherty Memorial Fund of AIME, Society of Petroleum Engineers **3** (1993).

61. Van Genuchten MT. A closed-form equation for predicting the hydraulic conductivity of unsaturated soils. *Soil Sci Soc Am J* **44**(5):892-898 (1980).

62. Mualem Y. A new model for predicting the hydraulic conductivity of unsaturated porous media. *Water Resour Res* **12**(3):513-522 (1976).

63. Krevor S, Pini R, Li B, Benson SM. Capillary heterogeneity trapping of CO_2 in a sandstone rock at reservoir conditions. *Geophys Res Lett* **38**(15):1-5 (2011).

64. Krevor S, Blunt MJ, Benson SM, Pentland CH, Reynolds C, Al-Menhali A, et al. Capillary trapping for geologic carbon dioxide storage–From pore scale physics to field scale implications. *Int J Greenhouse Gas Control* **40**: 221-237 (2015).

65. Doughty C. Investigation of CO_2 plume behavior for a large-scale pilot test of geologic carbon storage in a saline formation. *Transport Porous Med* **82**(1):49-76 (2010).

66. Suekane T, Nobuso T, Hirai S, Kiyota M. Geological storage of carbon dioxide by residual gas and solubility trapping. *Int J Greenhouse Gas Control* **2**(1):58-64 (2008).

67. Qi R, LaForce TC, Blunt MJ. Design of carbon dioxide storage in aquifers. *Int J Greenhouse Gas Control* **3**(2):195-205 (2009).

68. Stalker L, Varma S, Van Gent D, Haworth J, Sharma S. South West Hub: a carbon capture and storage project. *Aust J Earth Sci* **60**(1):45-58 (2013).

69. Al-Anssari S, Barifcani A, Wang S, Iglauer S. Wettability alteration of oil-wet carbonate by silica nanofluid. *J Colloid Interf Sci* **461**:435-442 (2016).